

Supplementary Information

for

Interaction Between Biimidazole Complexes of Ruthenium and Acetate: Hydrogen Bonding and Proton Transfer

Hao-Jun Mo, Jin-Ji Wu, Zheng-Ping Qiao and Bao-Hui Ye*

MOE Key Laboratory of Bioinorganic and Synthetic Chemistry, School of Chemistry and Chemical
Engineering, Sun Yat-Sen University, Guangzhou 510275, China

EMAIL: cesybh@mail.sysu.edu.cn

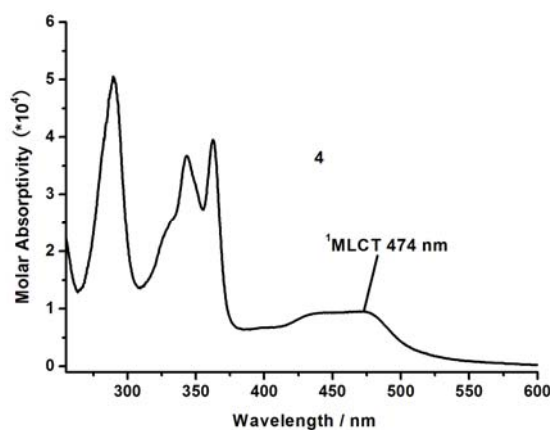


Fig. S1 Absorption spectra of **4** in acetonitrile at 298 K

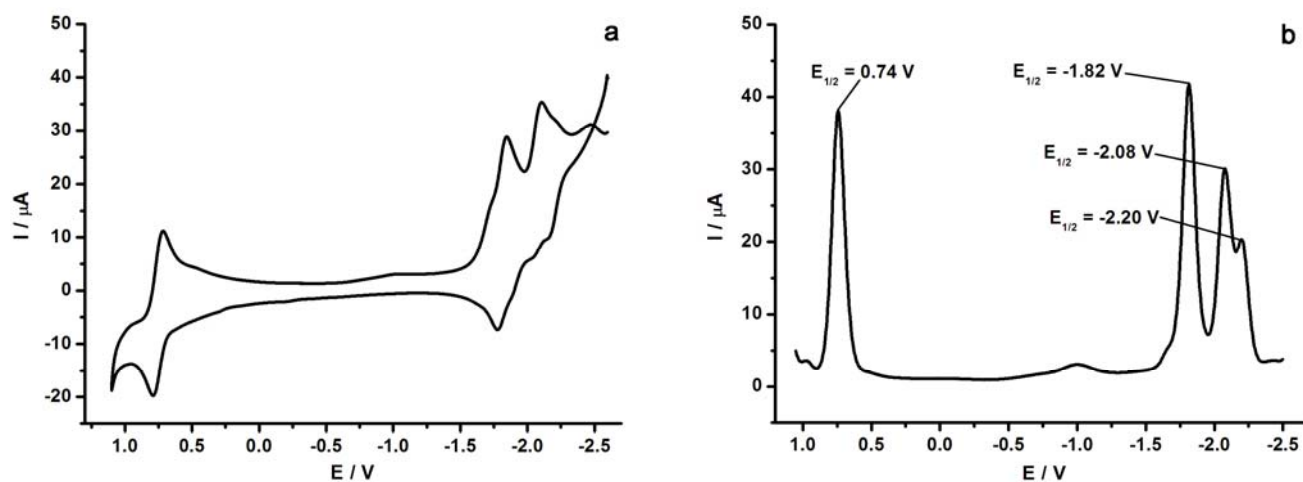


Fig. S2 (a) Cyclic voltammetric and (b) square wave voltammetric curves of **4** with a scan rate of $100 \text{ mV}\cdot\text{s}^{-1}$ in acetonitrile at 298 K (vs. Ag/AgNO_3).

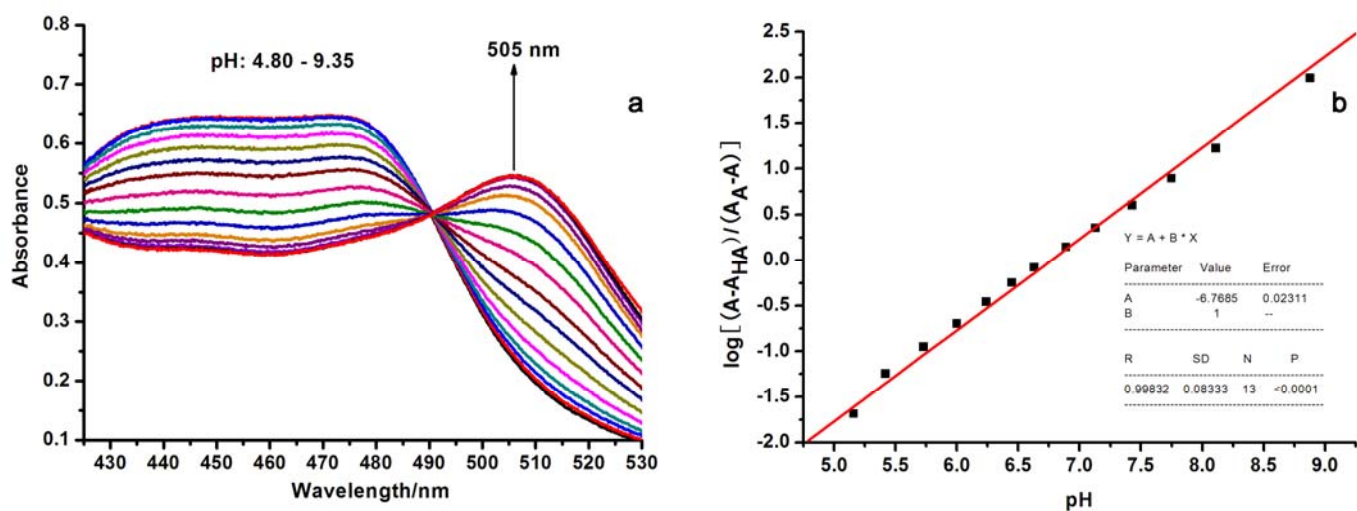


Fig. S3 Determination of pK_{a1} of **4** in acetonitrile-water mixture by UV method. (a) Absorption spectral change as pH value increases. (b) Linear fitting of pK_{a1} .

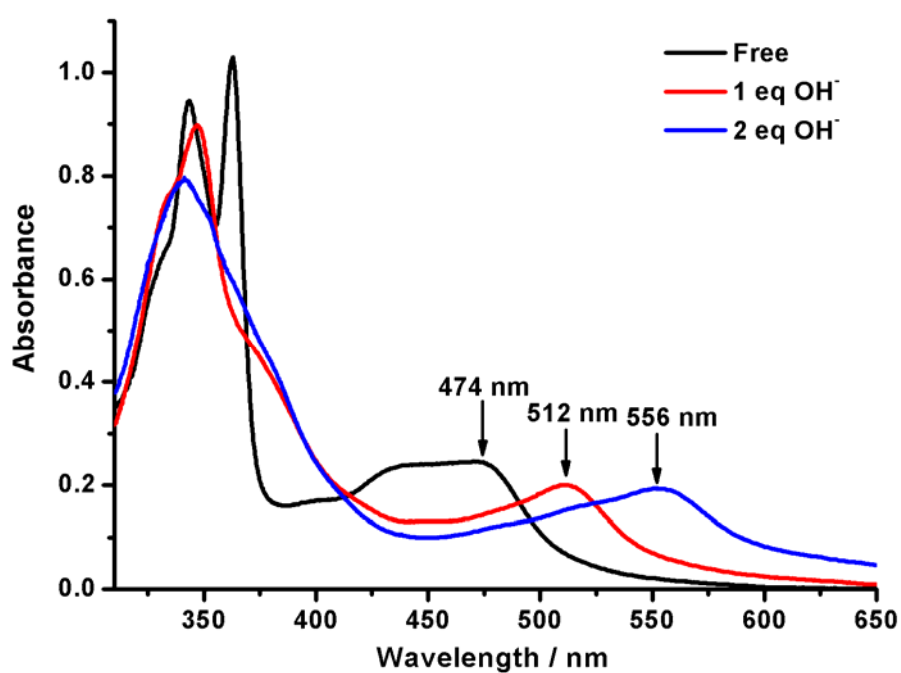


Fig. S4 Absorption spectra of **4** ($2 \times 10^{-5} \text{ mol} \cdot \text{dm}^{-3}$) in acetonitrile in the absence and presence of 1 equiv and 2 equiv of OH^- .

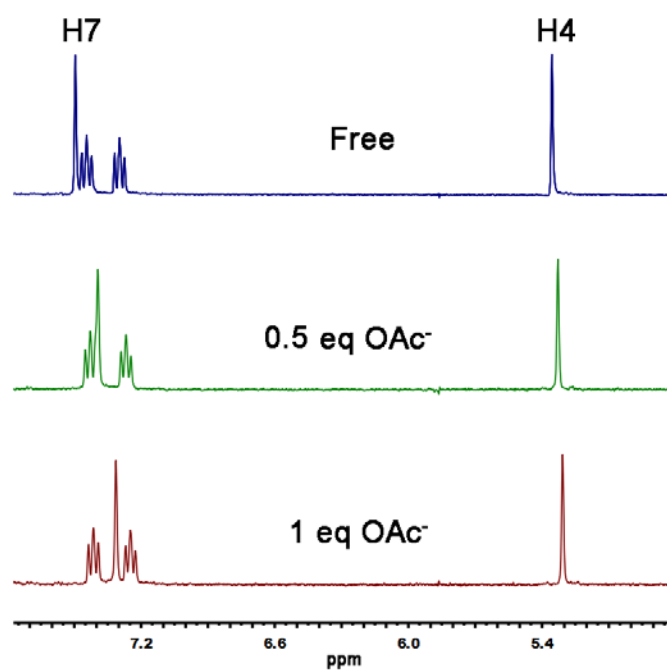


Fig. S5 ^1H NMR titration of **4** ($0.003 \text{ mol}\cdot\text{dm}^{-3}$) in acetonitrile- d_3 with OAc^- (298 K, 300 MHz).

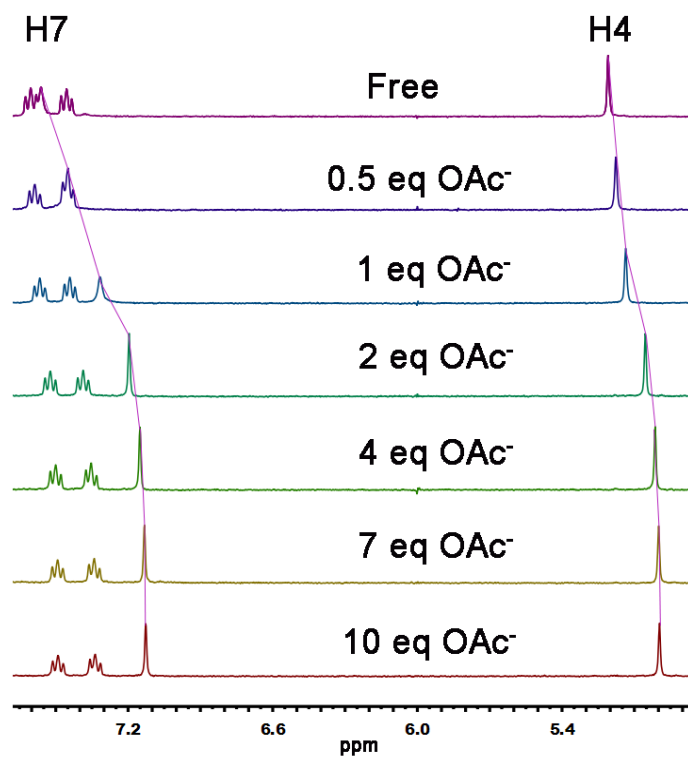


Fig. S6 ^1H NMR titration of **4** ($0.003 \text{ mol}\cdot\text{dm}^{-3}$) in $\text{DMSO}-d_6$ with OAc^- (298 K, 300 MHz).

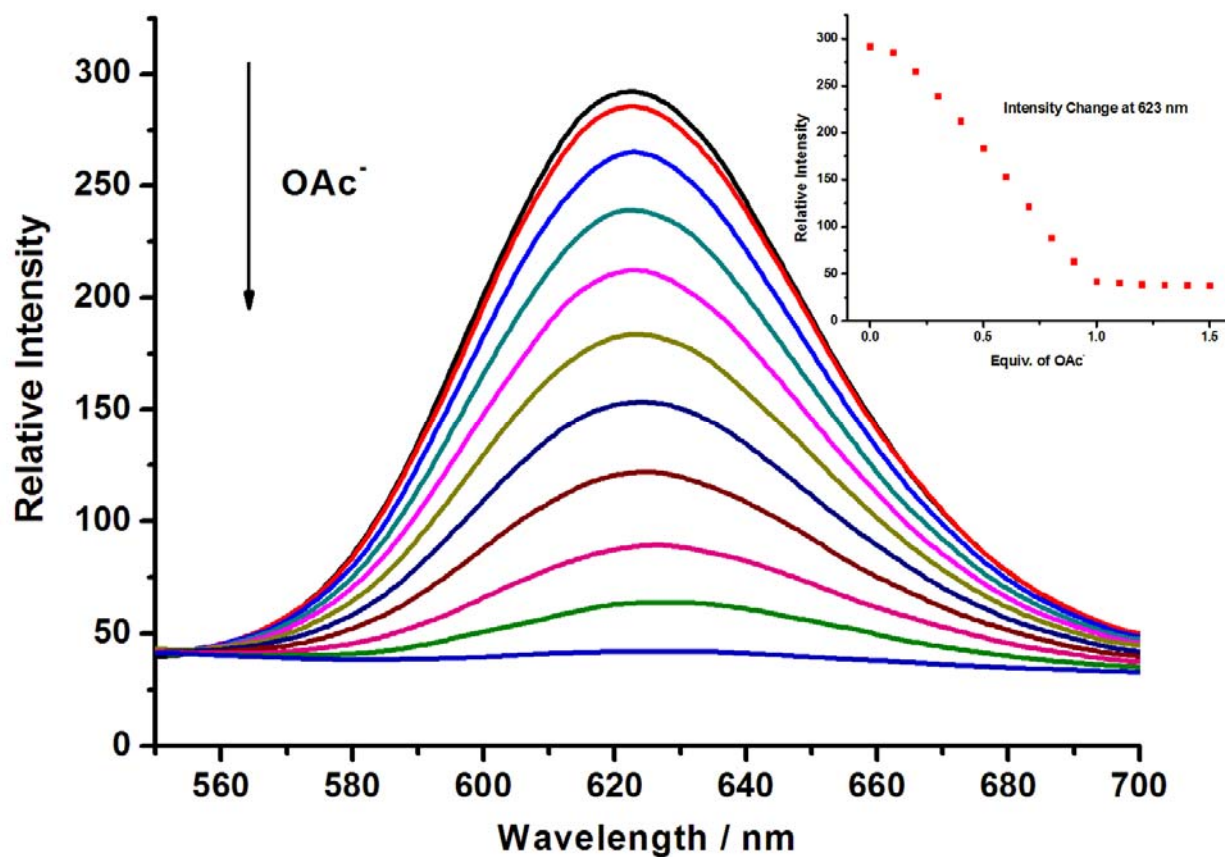


Fig. S7 Emission spectral response of **4** (2.0×10^{-5} mol·dm⁻³ in acetonitrile, 298K, $\lambda_{\text{ex}} = 470$ nm) upon addition of OAc⁻ anion. Inset: Intensity at 623 nm versus equiv of OAc⁻.

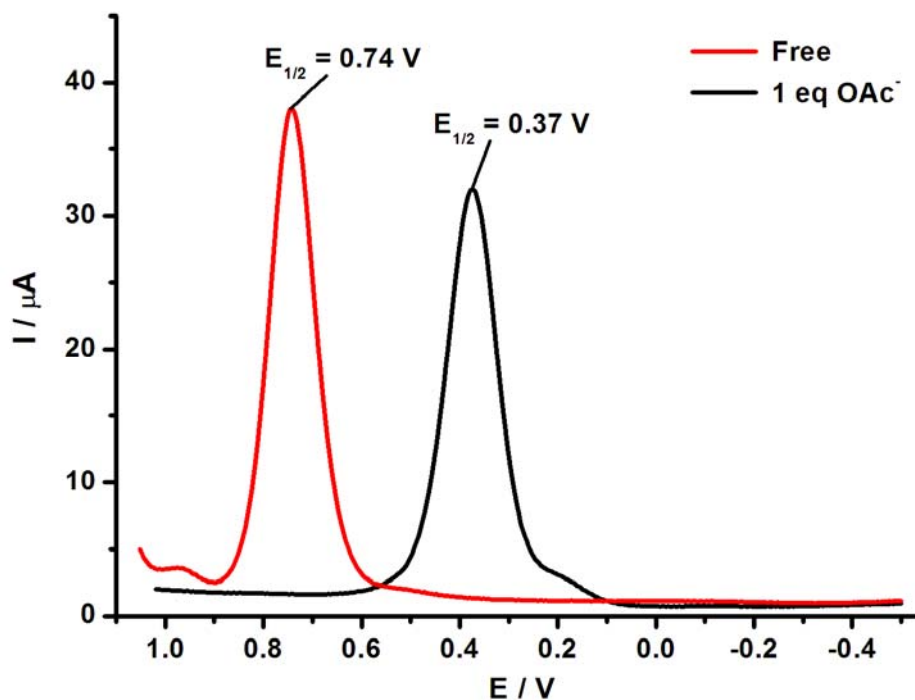


Fig. S8 SWV measurements of **4** in acetonitrile (0.001 mol·dm⁻³) in the absence and presence of 1 equiv of OAc⁻ (vs. Ag/AgNO₃).

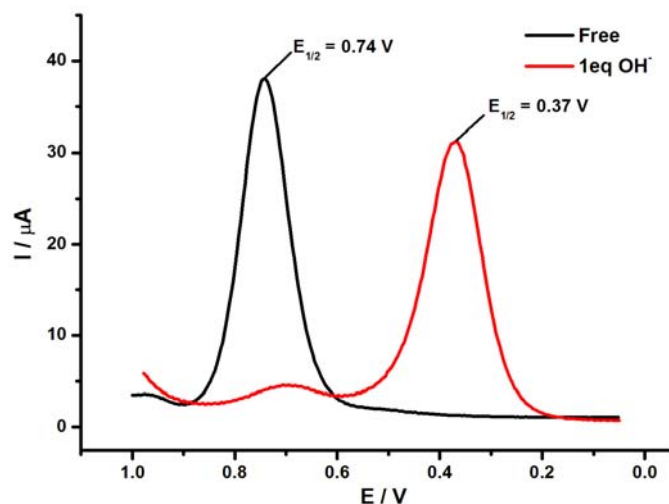


Fig. S9 SWV measurements of **4** in acetonitrile ($0.001 \text{ mol}\cdot\text{dm}^{-3}$) in the absence and presence of 1 equiv of OH^- (vs. Ag/AgNO_3).

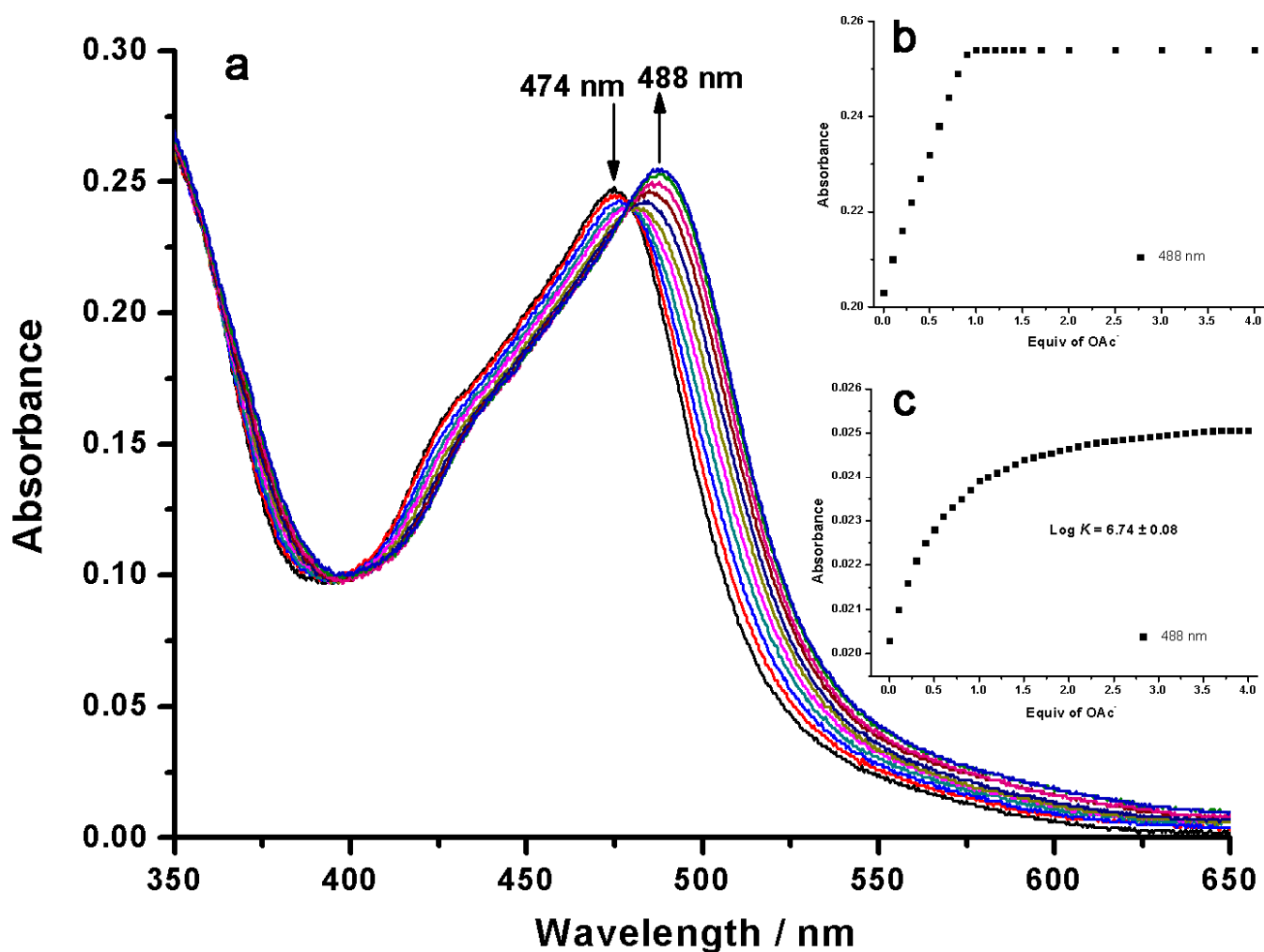


Fig. S10 (a) UV-vis titration of **1** ($2.0 \times 10^{-5} \text{ mol}\cdot\text{dm}^{-3}$) in acetonitrile in the presence of $0.0016 \text{ mol}\cdot\text{dm}^{-3}$ HOAc upon addition of OAc^- . Absorbance change at 488 nm for a $2.0 \times 10^{-5} \text{ mol}\cdot\text{dm}^{-3}$ solution (b) and for a $2.0 \times 10^{-6} \text{ mol}\cdot\text{dm}^{-3}$ solution (c) of **1**.

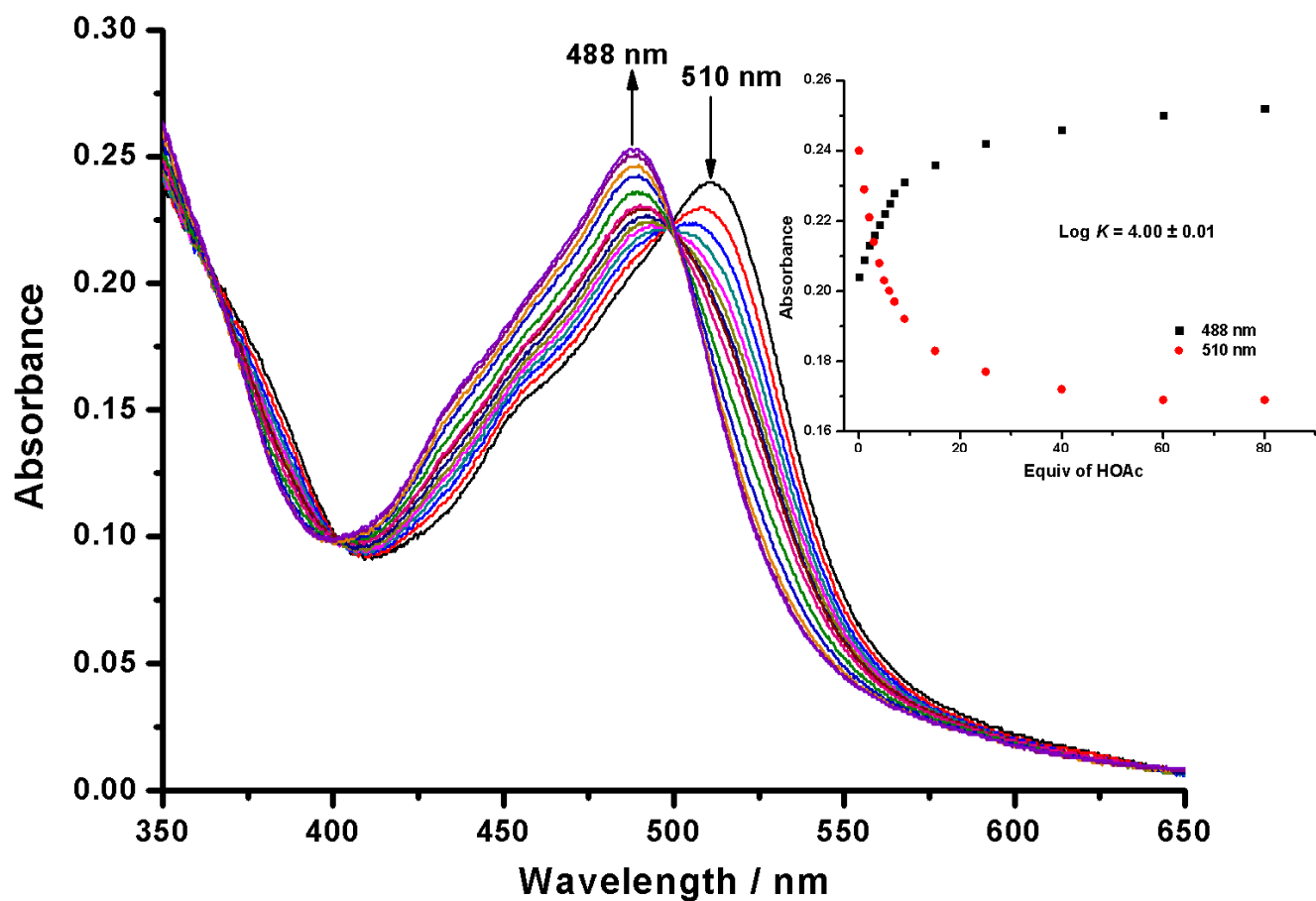


Fig. S11 UV-vis titration of mono-deprotonated **1** ($2.0 \times 10^{-5} \text{ mol} \cdot \text{dm}^{-3}$) in acetonitrile upon addition of HOAc. Inset: Absorbance at 488 and 510 nm vs. equiv of HOAc.

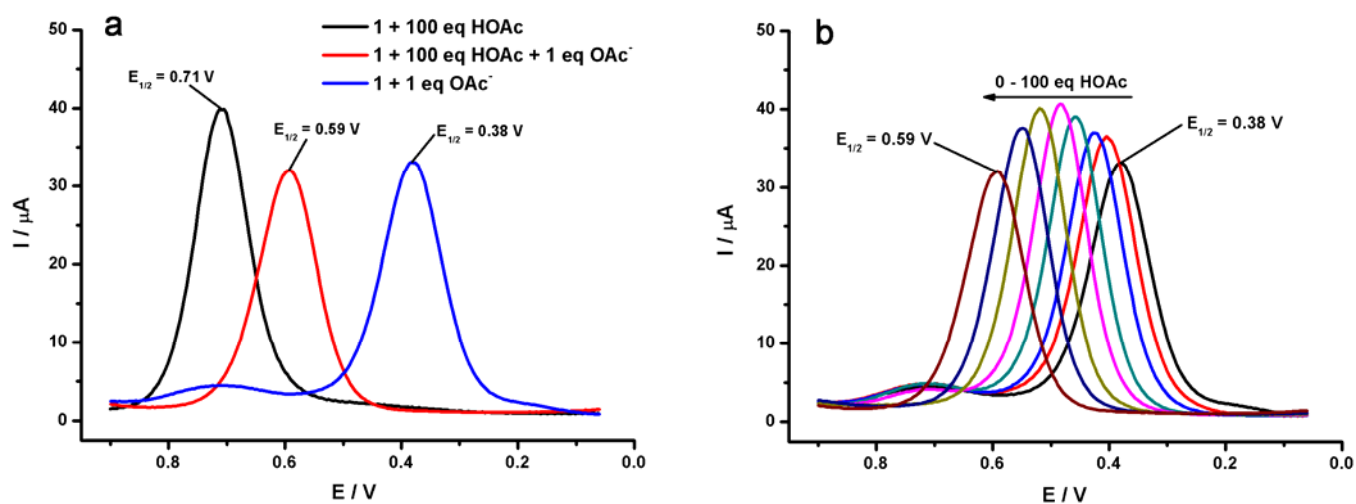


Fig. S12 (a) SWV curves of **1** ($0.001 \text{ mol} \cdot \text{dm}^{-3}$) and 100 equiv. of HOAc in acetonitrile in the absence and presence of 1 equiv. of OAc^- , and **1** in the presence of 1 equiv. of OAc^- . (b) Evolution of SWV curves of **1** ($0.001 \text{ mol} \cdot \text{dm}^{-3}$) and 1 equiv. of OAc^- in acetonitrile in the presence of increasing amount of HOAc from 0 to 100 equiv.

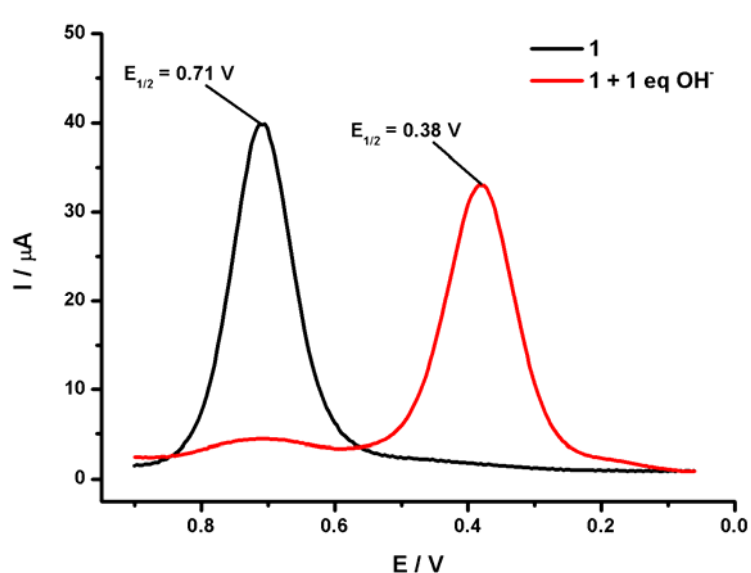


Fig. S13 SWV measurements of **1** in acetonitrile ($0.001 \text{ mol}\cdot\text{dm}^{-3}$) in the absence and presence of 1 equiv of OH^- (vs. Ag/AgNO_3).

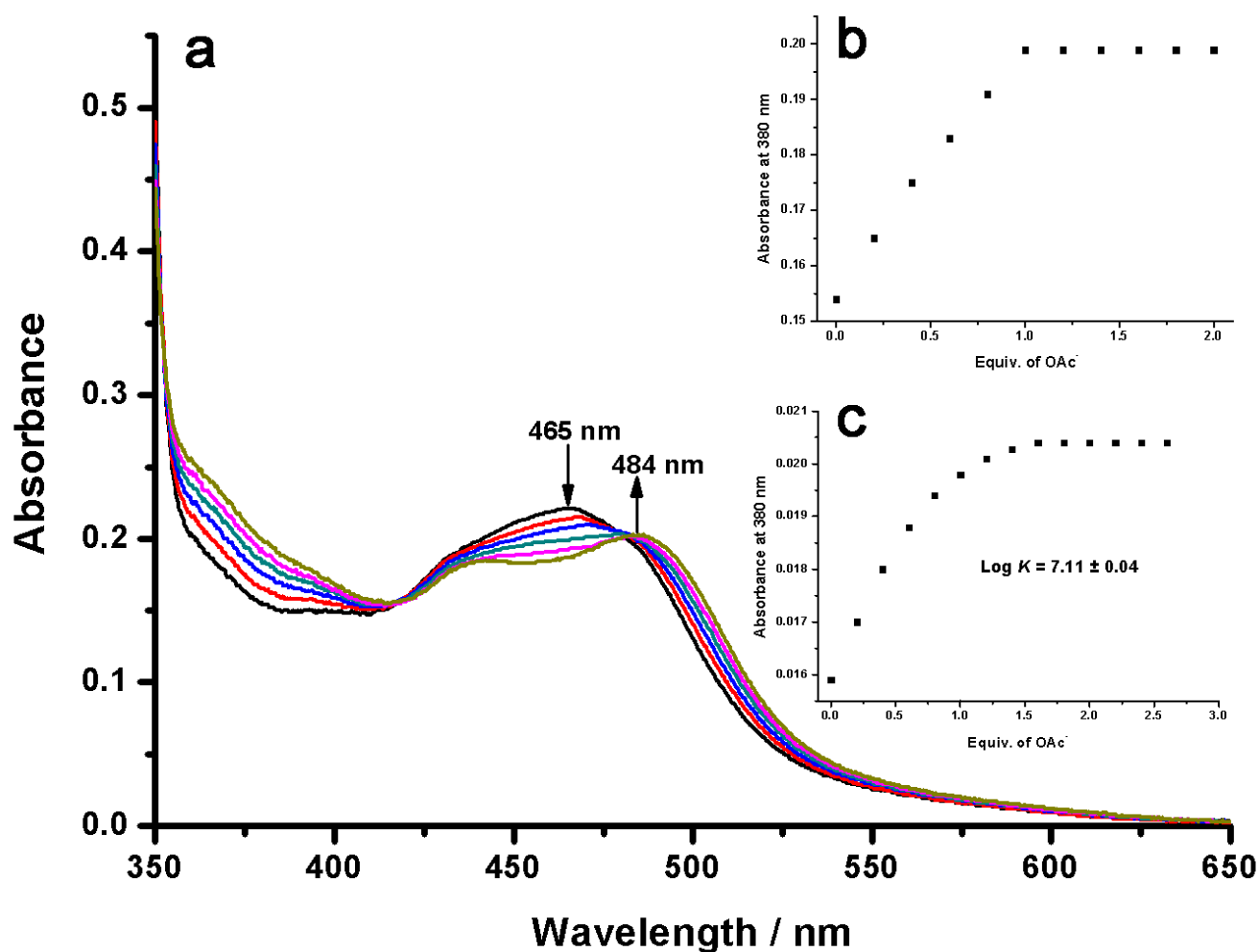


Fig. S14 (a) UV-vis titration of **2** ($2.0 \times 10^{-5} \text{ mol}\cdot\text{dm}^{-3}$) in acetonitrile in the presence of $0.048 \text{ mol}\cdot\text{dm}^{-3}$ HOAc upon addition of OAc^- . Absorbance change at 380 nm for a $2.0 \times 10^{-5} \text{ mol}\cdot\text{dm}^{-3}$ solution (b) and for a $2.0 \times 10^{-6} \text{ mol}\cdot\text{dm}^{-3}$ solution (c) of **2**.

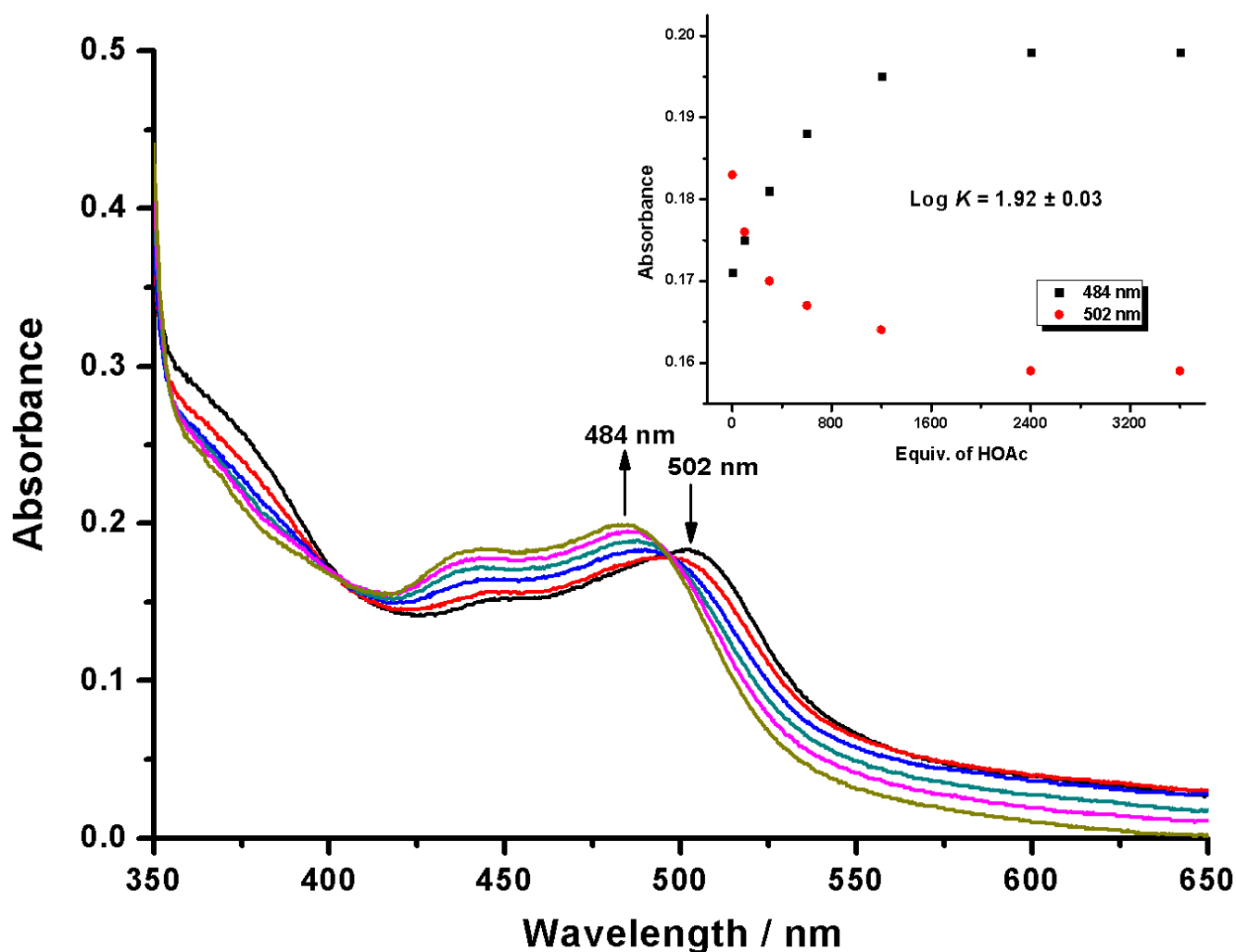


Fig. S15 UV-vis titration of mono-deprotonated **2** (2.0×10^{-5} mol·dm⁻³) in acetonitrile upon addition of HOAc. Inset: Absorbance at 484 and 502 nm vs. equiv of HOAc.

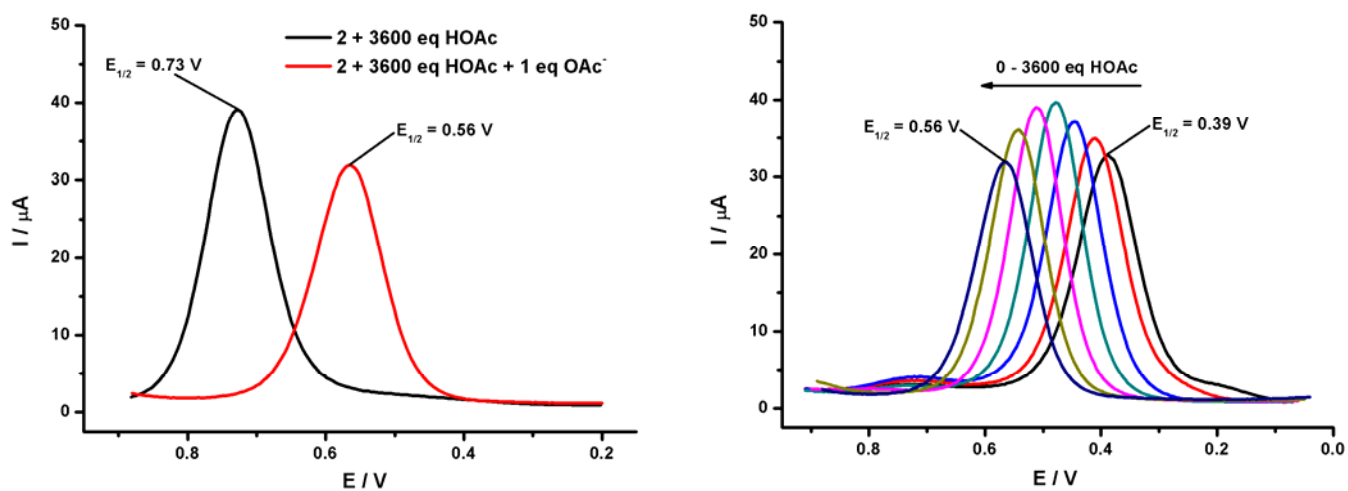


Fig. S16 (a) SWV curves of **2** (0.001 mol·dm⁻³) and 3600 equiv. of HOAc in acetonitrile in the absence and presence of 1 equiv. of OAc⁻. (b) Evolution of SWV curves of **2** (0.001 mol·dm⁻³) and 1 equiv. of OAc⁻ in acetonitrile in the presence of increasing amount of HOAc from 0 to 3600 equiv.

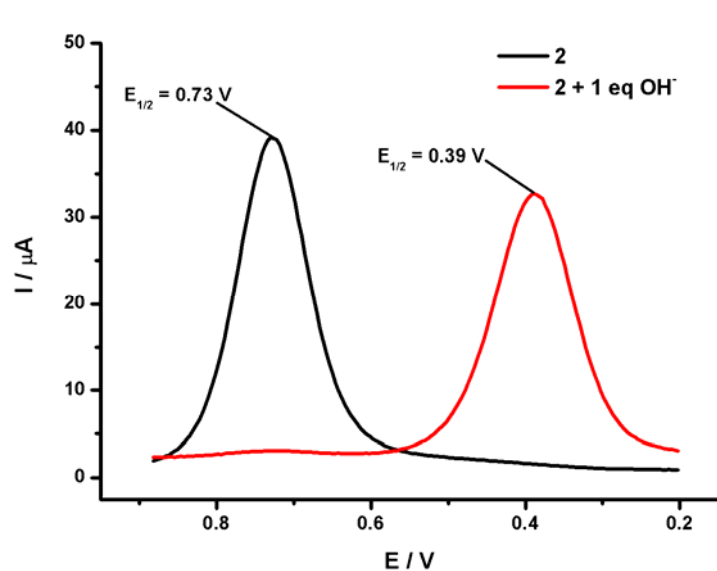


Fig. S17 SWV measurements of **2** in acetonitrile ($0.001 \text{ mol}\cdot\text{dm}^{-3}$) in the absence and presence of 1 equiv of OH^- (vs. Ag/AgNO_3).

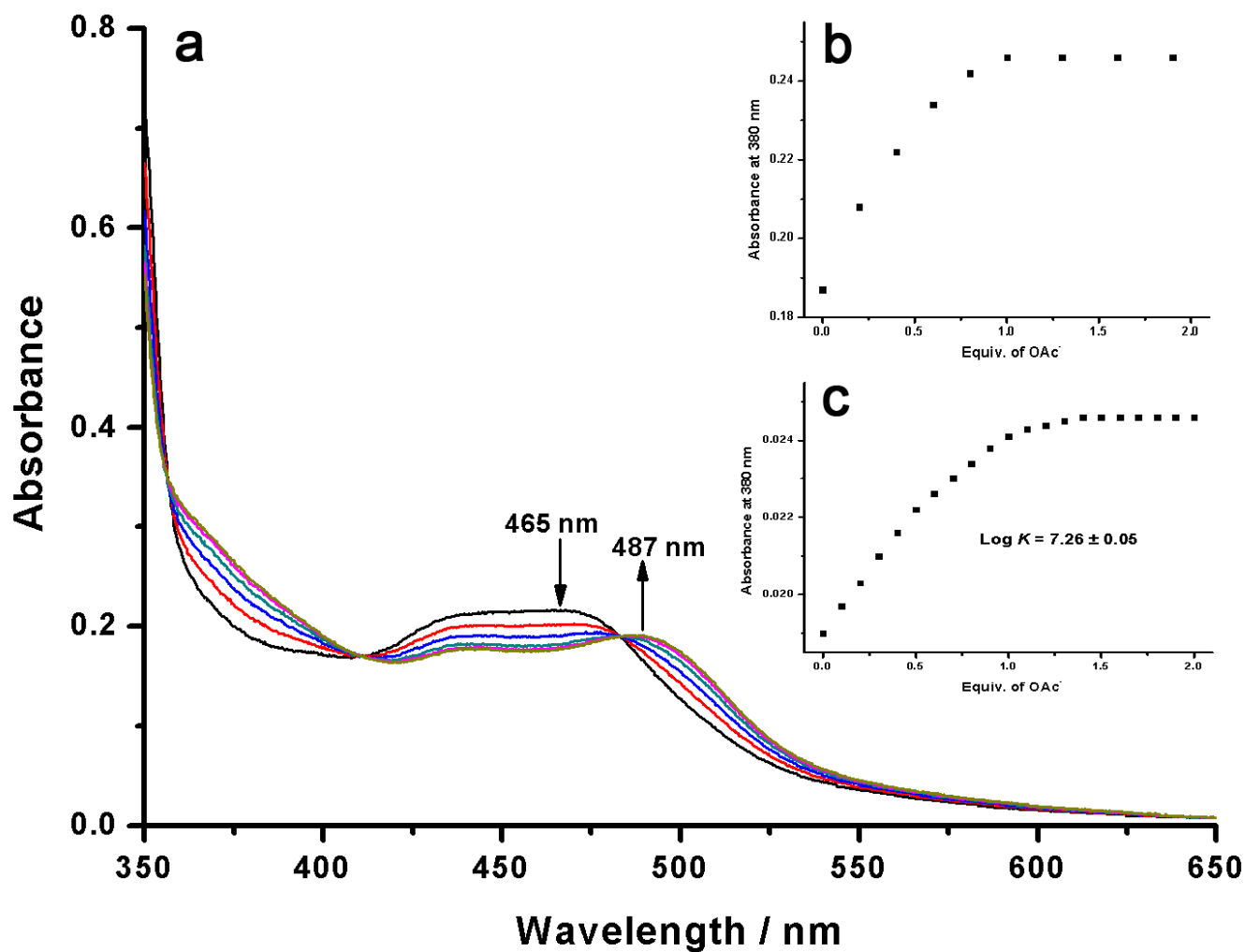


Fig. S18 (a) UV-vis titration of **3** ($2.0 \times 10^{-5} \text{ mol}\cdot\text{dm}^{-3}$) in acetonitrile in the presence of $0.009 \text{ mol}\cdot\text{dm}^{-3}$ HOAc upon addition of OAc^- . Absorbance change at 380 nm for a $2.0 \times 10^{-5} \text{ mol}\cdot\text{dm}^{-3}$ solution (b) and for a $2.0 \times 10^{-6} \text{ mol}\cdot\text{dm}^{-3}$ solution (c) of **3**.

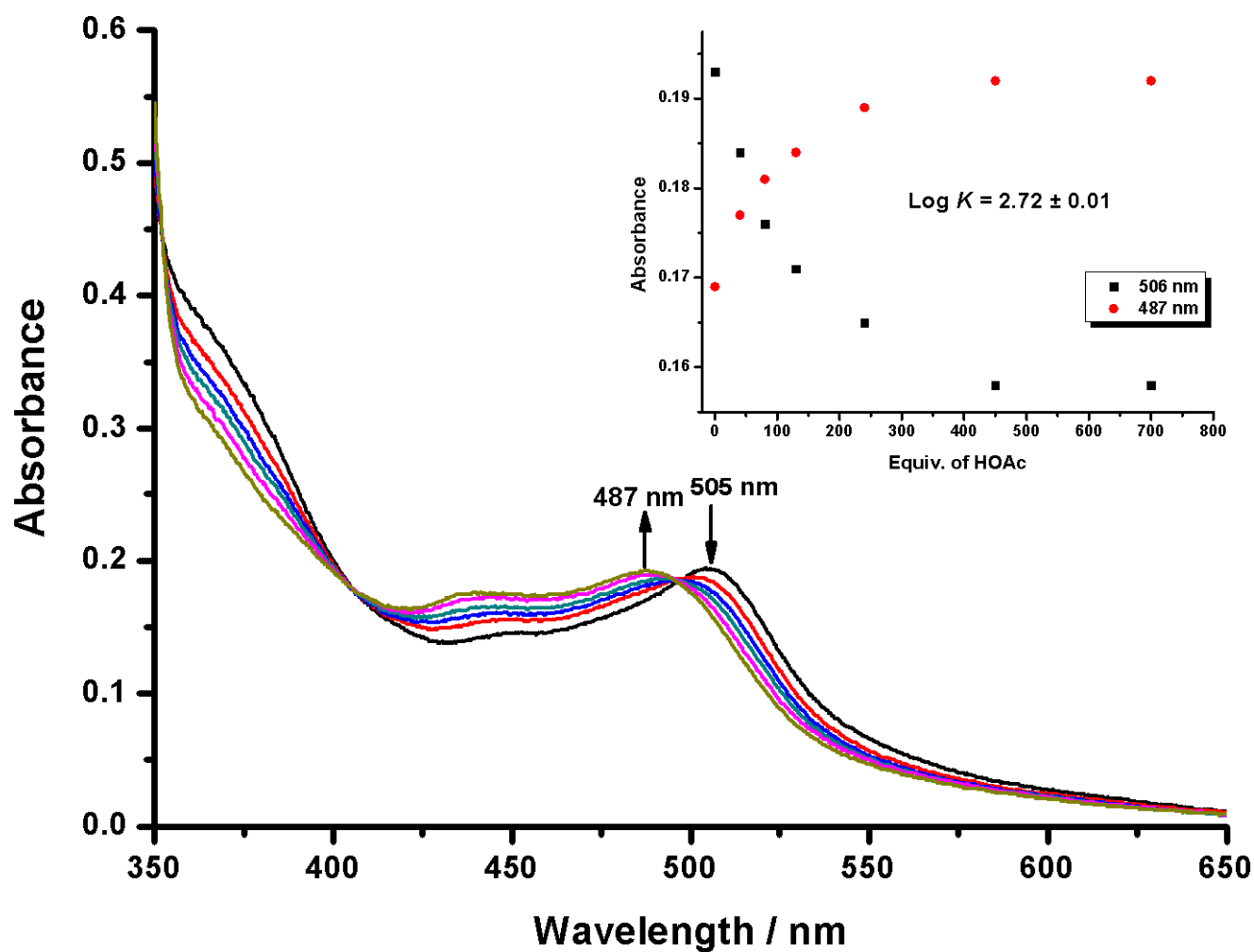


Fig. S19 UV-vis titration of mono-deprotonated **3** (2.0×10^{-5} mol·dm⁻³) in acetonitrile upon addition of HOAc. Inset: Absorbance at 487 and 505 nm vs. equiv of HOAc.

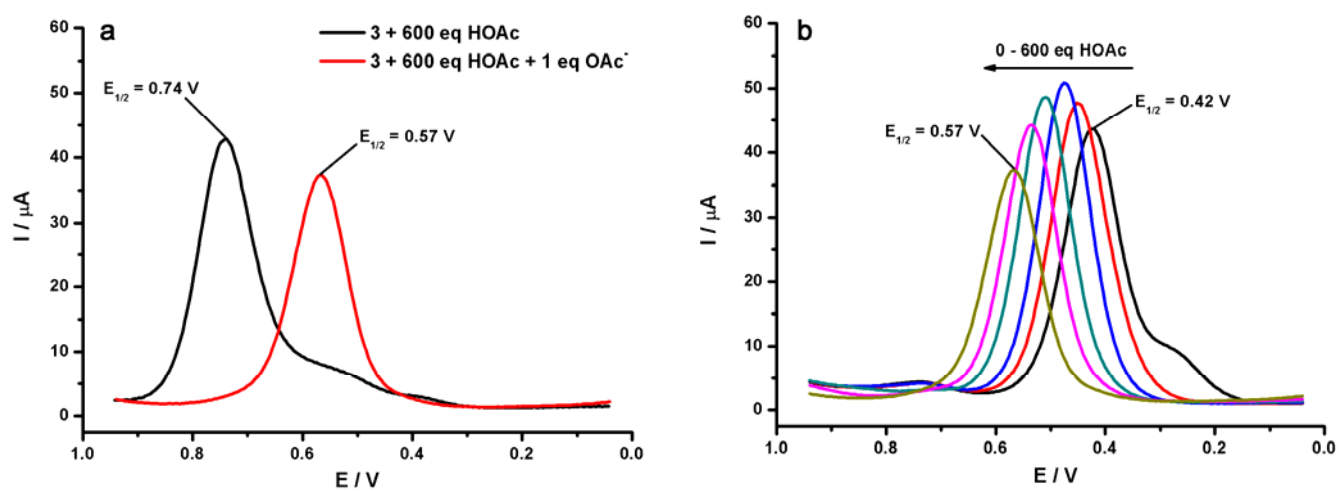


Fig. S20 (a) SWV curves of **3** (0.001 mol·dm⁻³) and 600 equiv. of HOAc in acetonitrile in the absence and presence of 1 equiv. of OAc⁻. (b) Evolution of SWV curves of **3** (0.001 mol·dm⁻³) and 1 equiv. of OAc⁻ in acetonitrile in the presence of increasing amount of HOAc from 0 to 600 equiv.

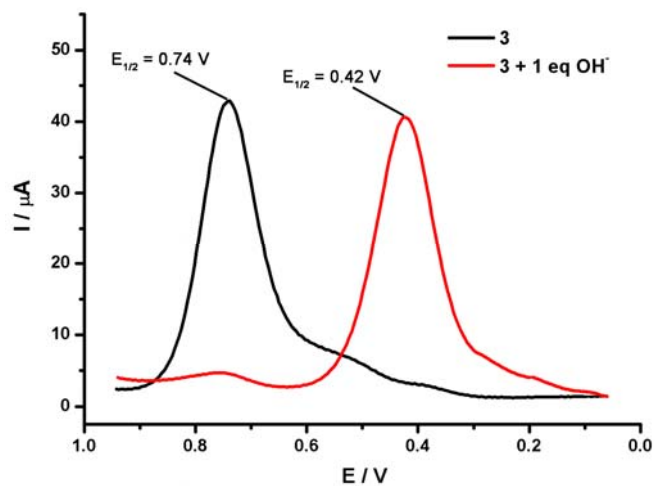


Fig. S21 SWV measurements of **3** in acetonitrile (0.001 mol·dm⁻³) in the absence and presence of 1 equiv of OH⁻ (vs. Ag/AgNO₃).

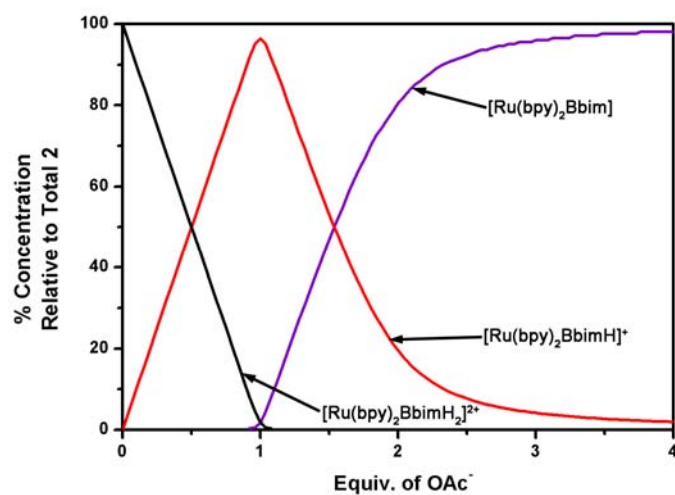


Fig. S22 Distribution diagram for **2** in acetonitrile upon addition of OAc⁻.

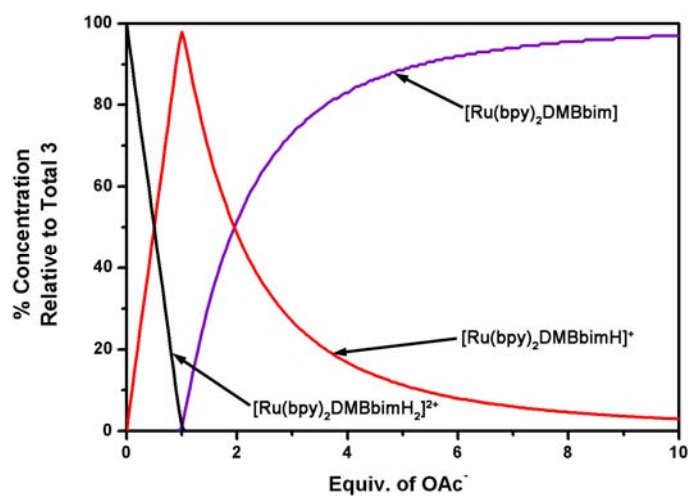


Fig. S23 Distribution diagram for **3** in acetonitrile upon addition of OAc⁻.